

Extracting the oscillatory component from thermokinetic time series in the H/Pd system¹

E. Lalik

*Jerzy Haber Institute of Catalysis and Surface Chemistry, Polish Academy of Sciences,
Niezapominajek 8, Krakow 30-239, Poland, E-mail: nclalik@cyf-kr.edu.pl*

Abstract

The mean value theorem for integrals has been applied in construction of a base curve for non-equilibrium thermokinetic oscillations. Following discretization of the experimental periodic time series to form segments that approximately correspond to the oscillatory period, the mean value was calculated for each of them. The values so obtained were interpolated and the new non-oscillatory curve so constructed turned out to have the properties enabling it to be used as a baseline for the oscillatory component of the original thermokinetic time series. Crucially, both the area under the new curve and that under the original time series were strictly identical. The pointwise subtraction of the new base from the original curve yields another oscillatory time series that may be considered as the oscillatory component extracted from the experimental thermokinetic data. The mathematical basics for the method has been outlined. Two experimental thermokinetic time series resulting from oscillatory sorptions of H₂ and D₂ in the metallic Pd powder has been analyzed using the procedure, showing certain new empirical aspects that could not have been found otherwise.

1. Introduction.

In most of experimental measurements of oscillatory behaviour, the resulting time series turn out to oscillate around the abscissa axis and it is therefore natural to consider the x-axis to be a base, or the zero-line for such oscillations. The oscillatory chemical reactions, however, do not oscillate in such a pendulum-like manner, since they occur far from equilibrium.¹ Likewise, the thermokinetic oscillations proceeds in systems that usually remains far from equilibrium throughout the experiment and so the calorimetric time series so recorded may be running entirely above the abscissa axis, if the reaction is exothermic (cf. Figure 1 A and B). In spite of this upward shift, the frequency of such time series may be readily determined by usual Fourier transforming.^{2,3} Yet their amplitude may be difficult to establish, since there is no obvious baseline for them to be used. Also, the very notion of the exothermic vs. endothermic peaks become ambiguous, in fact, one can only talk about a periodic variations of exothermicity. To conclude about the amplitude, therefore, a transformation needs to be applied in order to extract the oscillatory component in a way to have them oscillating around the zero axis, with the latter to be used as baseline.

In the current article, we report on a method devised for finding a base curve along such non-equilibrium oscillatory time series that would play the role of zero-line, yet not be identical with the abscissa axis. We seek to construct a curve that would model a “flat”, averaged rate of heat evolution in oscillatory reaction, in such a way as to be possibly used as a virtual base-line for the thermokinetic oscillations actually recorded. The construction is based on mean values, in the sense of the mean value theorem for integrals, found individually for each separate period of oscillations and subsequently interpolated to form the required curve.

¹ The following article has been submitted to Chaos: An Interdisciplinary Journal of Nonlinear Science

Mathematically, the procedure begins with discretization of the experimental time series, using the inflection points as the time limits for the ensued segments, each covering an extent of time roughly corresponding to oscillation period, followed by applying the integral mean value theorem to each of these segments separately. The so calculated mean values may be then used as a set of fit points to define a new, non-oscillatory curve (cf. Figures 1 A and B, blue line), purportedly the model for the hypothetical “flat” heat evolution. As a matter of validation, both the modeled flat base-line and the experimental oscillatory time series have to yield the same areas on integration (cf. Figures. 1 A and B), because the total heat of reaction has to be conserved, irrespective of whether oscillatory or not. The pointwise subtraction of the two lines, in turn, yields yet another oscillatory curve that represents the oscillatory component extracted from the original thermokinetic time series. The total area under this extracted oscillatory curve must be zero and, as it turns out, it also preserves the basic topology of the original data (cf. Figures 1 D).

In illustrating this method, we employ the results of two experiments with the oscillatory sorption of hydrogen or deuterium in the Pd powder. The observations of thermokinetic oscillations accompanying the process of sorption of H_2 or D_2 in metallic Pd was reported previously in refs. 2-5. Detection of oscillations was enabled by adding a 10 % admixture of an inert gas (N_2 , He, Ne, Ar, Kr) to the flow of $H_2(D_2)$ prior to its contact with Pd powder. While the inert admixture has been crucial for the thermokinetic oscillations to be observed, the area under the time series recorded has been strictly invariant, with the heat evolved always in agreement with the standard thermodynamic heat of the process.^{2,3} Nevertheless, the oscillation frequency turned out to be a linear function of the first ionization potential and the square root of atomic mass of the inert gas actually used as the admixture to $H_2(D_2)$.³ Here we report that the extraction of the oscillatory component of the thermokinetic oscillations recorded in the $H_2/N_2/Pd$ and $D_2/N_2/Pd$ systems reveals new features that could not have been observed before. We further discuss this findings in terms of both their mathematical and physical significance.

2. Experimental.

The coarse grained palladium powder (purity 99.999%, particle size 0.25–2.36 mm), used for the sorption of H_2 , and the fine grained Pd powder of granularity less than 75 μm , used for the sorption of D_2 , have both been supplied by Aldrich Co.. The following gases: nitrogen (99.999%), hydrogen (99.999%) and deuterium (99.9 %) were provided by Linde Gas Poland S. A. A Microscal gas flow-through microcalorimeter, model FMC 4110, has been used for experiments. The design and operation of this instrument has been described in detail in ref. 6. The experimental procedure leading to periodic oscillatory sorption of $H_2(D_2)$ in Pd has been described in detail in ref. 2 and 3. The instrument measures the rate of heat evolution accompanying a solid–gas interaction under isothermal conditions. A sample of Pd powder is placed in a minute microcalorimetric cell (7 mm in diameter, ca. 0.15 cm³ in volume) and the measurement is carried out in a flow-through mode. The cell is located centrally within a much larger metal heat sink. The latter ensures a steady removal of the total of evolving heat and prevents its accumulation within the cell. As a reaction is running within the cell, a minute difference of temperatures, between the vicinity of the cell and the locations closer to

the outer edge of heat sink, can be measured continuously by a system of thermistors, appropriately located within the latter. The oscillatory kinetics arises after a short initial period of the exposure of Pd powder to $\text{H}_2(\text{D}_2)/\text{N}_2$ mixture and ceases on saturation of the sample after ca. 20 - 30 min (cf. Figures 1A and B), i.e., on reaching the state of dynamic equilibrium between the hydride and the $\text{H}_2(\text{D}_2)$ in the gas phase. The raw time series are further processed using a calibration factor (CF), obtained for each experiment by *in situ* calibration, to yield the final calorimetric curve representing the rate of heat evolution vs. time.

3. Outline of the concept and its application.

3.1. Construction of the mean value curve. We will apply the mean value theorem for integrals to our experimental thermokinetic time series $q(t)$ following a discretization procedure. The latter consists of dividing of the whole time series into segments approximately corresponding to the periods of oscillations. Having found the mean value for each segment, we used them to construct a new curve, further referred to as the mean value curve.

The mean value theorem states, that for a function $f(x)$ which is continuous and real-valued within an interval $[a,b]$, there exists a value $c \in (a,b)$ such, that the product $f(c)(b - a)$ equals to the area under the $f(x)$ curve within the (a,b) interval (cf. Figure 2):⁷

$$f(c)(b - a) = \int_a^b f(x)dx \quad (1)$$

Consider the experimental thermokinetic oscillations $q(t)$ represented in Figure 1A or B (the red lines). After having it divided into a range of segments, we now consider each segment of this time series as a continuous function $q(t)$, $q: [t_1, t_2] \rightarrow \mathbb{R}$, but in addition we also assume that $q(t)$ is twice differentiable within the interval $[t_1, t_2]$. The latter condition is necessary, since the limits t_1 and t_2 , are each determined as the inflection points in the ascending parts of the oscillatory curve $q(t)$, marked by the red dots in Figure 1 C. Their positions correspond of the points for which the second time derivative is zero, $d^2q/dt^2 = 0$ (cf. cyan line in Figure 1 C) and the first time derivative dq/dt has a maximum (not shown). With the limits t_1 and t_2 so defined, each segment approximately corresponds to a single period of oscillations. Using those points as the integral limits, a function mean value $M = q(t_M)$ can be determined for each individual segment:

$$M = \frac{1}{t_2 - t_1} \int_{t_1}^{t_2} q(t)dt \quad (2)$$

Apart from the M value, one needs also to determine its abscissa t_M , in order to gain a fit point (t_M, M) for the mean value curve. The mean value theorem guarantees that the value M must be somewhere in the segment of the experimental time series between $q(t_1)$ and $q(t_2)$, but it does not determine its abscissa t_M , only saying that $t_M \in (t_1, t_2)$. Ideally, one could determine t_M for all segments. However, it would be inefficient to try to find all the t_M values in all segments one by one manually. Instead, as a more practical approach, we approximate the abscissa of M as the midpoint between t_1 and t_2

$$t^*_i = (t_{2i} - t_{1i})/2 \quad (3)$$

This is illustrated in Figure 1 C. Effectively, using formula (3) recurrently in each i th segment, we define a series of midpoints having coordinates $(t^*_1, M_1), (t^*_2, M_2), \dots (t^*_n, M_n)$,

corresponding to the succession of segments, from 1 to n (cf. blue dots in Figures 1 A and B, the mean values are also listed in Tables I and II). These points are evenly distributed, separated by an extent of time approximately corresponding to the oscillation period (cf. blue dots in Figure 1 D). In general, they lay close, but not exactly on the curve $q(t)$. Using them as fit points for interpolation produces a new (non-oscillatory) curve $h(t)$, running midway across the calorimetric time series (cf. the blue lines in Figures 1A, B and D). As the values t^* are used to approximate the values t_M , therefore the curve $h(t)$ (based on t^* values) is an approximation of the proper mean value curve (that would be based on t_M values). Now we need to test how good this approximation is.

The validity of the approximation of the mean value curve by the curve $h(t)$ can be confirmed both experimentally and mathematically. The experimental evidence consists of checking whether the areas under the curves $q(t)$ and $h(t)$ are equal. Physically, the mean value curve represents a hypothetical time-evolution of heat that the system would produce if the reaction proceeded in a non-oscillatory manner, under the reaction conditions otherwise identical to those of the oscillatory process. As a “sanity check”, to assess the closeness of the $h(t)$ approximation, a condition has to be used, that the total heat evolution represented by the area under this hypothetical non-oscillatory curve must be equal to that under the actual oscillatory time series. Indeed, the integration confirms that these areas are practically equal, found to be 35652 and 35643 mJ, respectively under the curves $q(t)$ and $h(t)$ in the sorption of deuterium in Pd (cf. Figure 1 A) and, similarly, 27976 and 27970 mJ in the sorption of hydrogen (cf. Figure 1 B). Thus the experiments confirm the validity of using the curve $h(t)$ as approximation of the mean value curve. This finding also confirms experimentally the validity of using formula (3), i.e., the approximation of t_M by t^* . We will further analyze the mathematics behind using formula (3) in Section 3.3.

3.2. Extracting the oscillatory component by the pointwise subtraction of $h(t)$ from $q(t)$.

The pointwise subtraction of the mean value curve $h(t)$ from the thermokinetic oscillations $q(t)$ yields a new oscillatory curve $g(t) = q(t) - h(t)$. Figure 1 D illustrates this operation for an enlarged fragment comprising three successive segments of the thermokinetic oscillations. The blue dots represents the corresponding three mean value points approximated with formula (3). Figures 1 E and F shows two examples of such pointwise subtraction for the entire experimental time series recorded in the sorption experiments in the Pd/D₂/N₂ (Figure 1 E) and the Pd/H₂/N₂ system (Figure 1 F). To achieve an effect of juxtaposition, the new $g(t)$ curve is shown as a fill plot representing oscillations around the zero baseline, against the original time series $q(t)$. An important requirement to be satisfy, while carrying out the numerical interpolation of the mean values M , is that the number of points in the resultant $h(t)$ curve must be equal to that in the experimental $q(t)$ time series. It is clear, that the pointwise subtraction preserves the frequency of thermokinetic oscillations. Hence, the $g(t)$ curve represents the extracted oscillatory component of the original thermokinetic time series $q(t)$. Expectedly, since the areas under $q(t)$ and $h(t)$ are identical, the total area under the curve $g(t)$ should be zero and this is indeed the case. This aspect will be discussed in more detail in Section 3.4 (cf. also Figure 4).

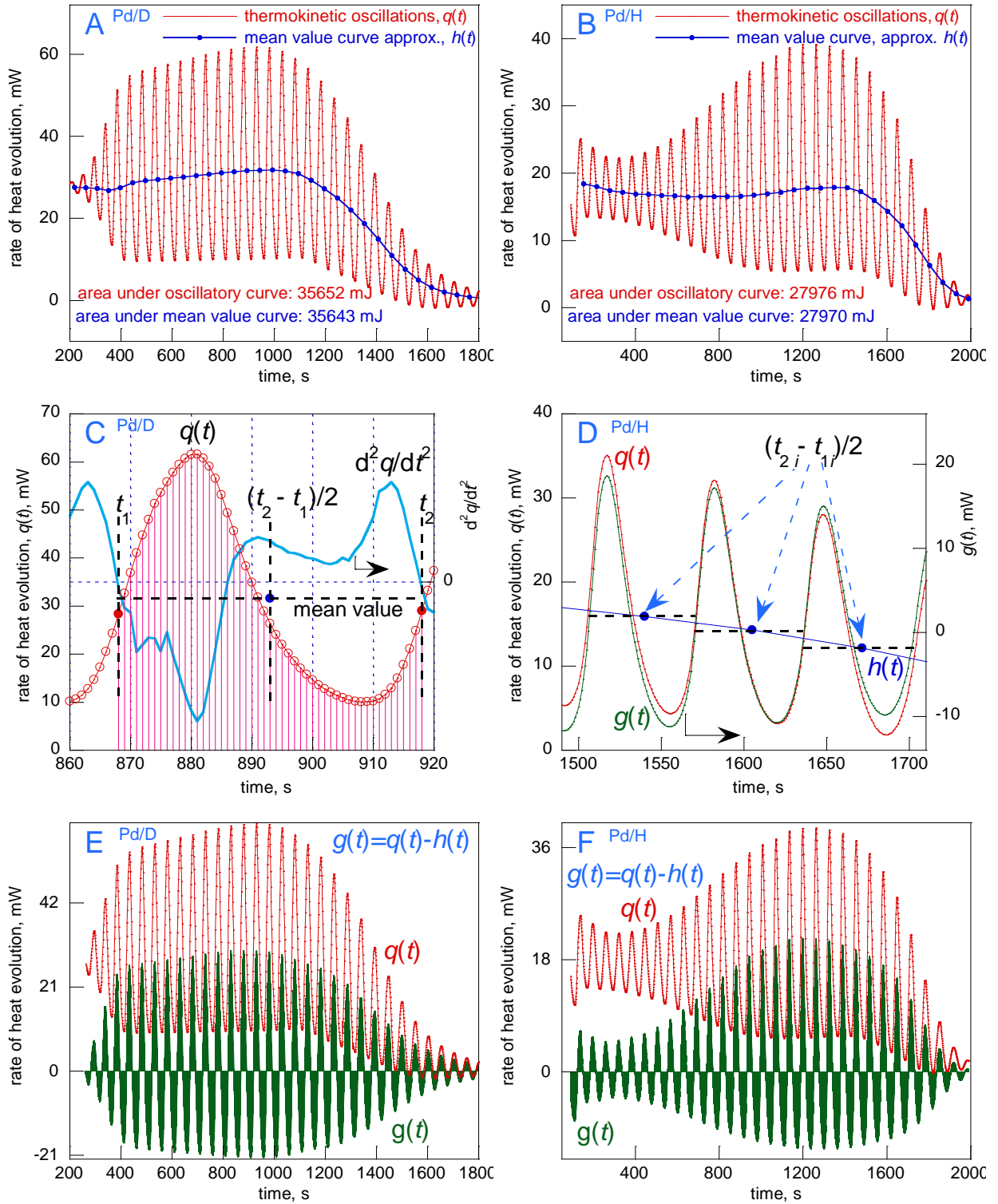


Figure 1. **A** and **B**): The approximated mean value curves $h(t)$ plotted against the thermokinetic oscillations $q(t)$, recorded, respectively, in Pd/D₂/N₂ and Pd/H₂/N₂ sorption experiments. **C**): A single segment has its limits at inflection points t_1 and t_2 (red dots) identified with the zeros of the second derivative d^2q/dt^2 curve (cyan). The fit point (blue dot), for the curve $h(t)$ to pass through, is established at the center, $(t_2 - t_1)/2$. **D**): A succession of three mean value fit points (blue dots), shown against the ensuing oscillatory curve $g(t) = q(t) - h(t)$. Note, that $g(t)$ (green) is plotted against y2 axis, shifted with respect to y axis, but of the same scale. **E** and **F**): The extracted oscillatory curves $g(t)$ (filled green) retain the original frequency of $q(t)$.

3.3. Mathematical underpinning of using formula (3). (Remark on notation: To avoid an excessive use of subscripts in the integration limits, for the sake of visual clarity of equations, the letters a , b and c are used in this section (also in Figure 2), instead of, respectively, t_1 , t_2 and t_M used elsewhere in this work.)

Mathematically, using formula (3) to approximate the positions of mean values can be justified by the following reasoning. Rewriting equation (1) we obtain

$$\int_a^c f(x)dx - f(c)(c - a) = - \int_c^b f(x)dx + f(c)(b - c). \quad (4)$$

Point c divides the interval (a,b) into two partitions (a,c) and (c,b) (cf. Figure 2). Formula (4) shows, that the area between the curve $f(x)$ and the line $y = f(c)$ over the partition (a,c) and the area between those lines over the partition (c,b) are equal in absolute value, but opposite in sign (cf. cyan shading in Figure 2). It can be shown, however, that such relation holds for any point that lays on the line $y = f(c)$ over the interval (a,b) , i.e., having an abscissa $d \in (a,b)$, shifted from c by any $|\Delta c|$. Splitting the definite integrals in (4) we obtain:

$$\int_a^d f(x)dx + \int_d^c f(x)dx - f(c)(c - a) = - \int_d^b f(x)dx + \int_d^c f(x)dx + f(c)(b - c) \quad (5)$$

After subsequent addition to both sides of (5) the terms $-f(c)d$ and $f(c)c$ and after cancellation we have

$$\int_a^d f(x)dx - f(c)(d - a) = - \int_d^b f(x)dx + f(c)(b - d) \quad (6)$$

which can be rewritten as

$$\int_a^d f(x)dx - f(c) \int_a^d dx = - \int_d^b f(x)dx + f(c) \int_d^b dx \quad (7)$$

or

$$\int_a^d [f(x) - f(c)]dx = - \int_d^b [f(x) - f(c)]dx. \quad (8)$$

The arbitrary point $d \in (a,b)$ divides the interval (a,b) into two partitions, (a,d) and (d,b) . The areas enclosed between the curve $f(x)$ and the line $y = f(c)$ within those intervals, respectively, represented by LHS and RHS of (8), are equal in absolute value, but opposite in sign.

The relation (8) holds irrespective of selection of d . It follows, that the definition of t^* according to formula (3) does not violate the conditions of the mean value theorem (1), in fact, t^* is a special case of $d = (b - a)/2$. Hence, the mean value M once calculated using formula (2), defines a horizontal line, that, technically speaking, can be used as a lifted x -axis from which to integrate the function $q(t)$.

It can further be shown, that both sides of (8) attain maximum for $x = c$. To see this, note, that since d can be selected anywhere within the interval (a,b) , the expression (8) can be rewritten using the integrals with variable upper limit u , instead of the fixed d

$$\int_a^u [f(x) - f(c)]dx = - \int_u^b [f(x) - f(c)]dx \quad (9)$$

or

$$\int_a^u [f(x) - f(c)]dx = \int_b^u [f(x) - f(c)]dx \quad (10).$$

Now we differentiate both side with respect to u and equate the result to zero,

$$\frac{d}{du} \int_a^u [f(x) - f(c)] dx = \frac{d}{du} \int_b^u [f(x) - f(c)] dx = 0 \quad (11)$$

yielding $f(x) = f(c)$, which is only true for $x = c$.

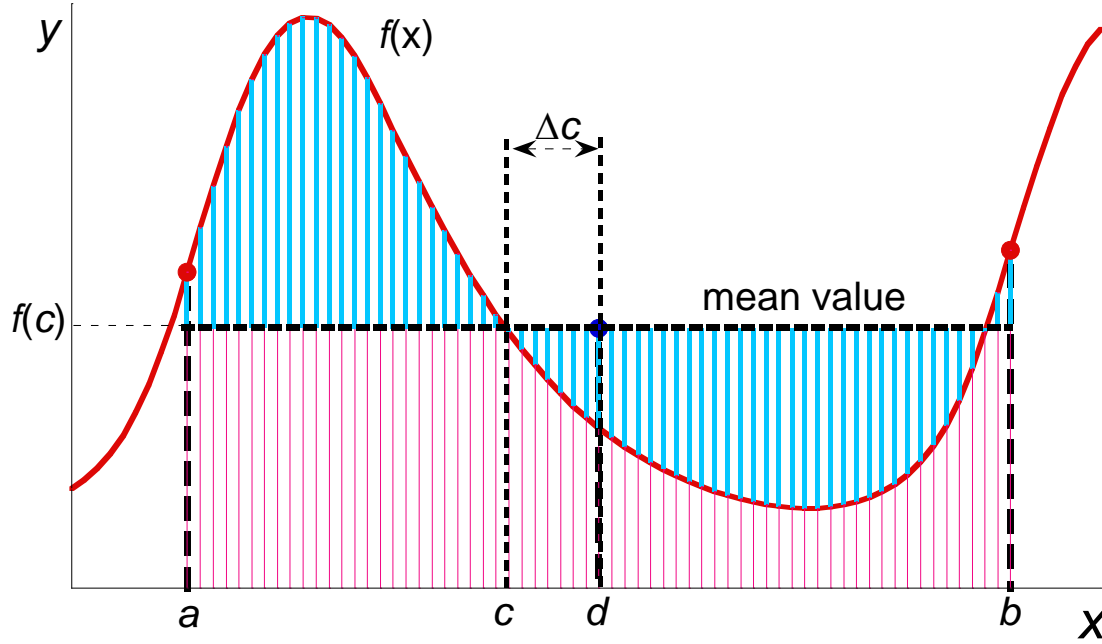


Figure 2. The mean value theorem for integrals (equation(1)) makes it possible to find a mean value point $f(c)$ that exists in the segment of the curve $f(x)$ over the interval (a, b) , but it does not determine its abscissa c . The cyan-shaded partitions above and below the mean value $f(c)$ are equal, irrespective of whether the division point for the segment (a, b) is c or d . The relation (8) shows that the same holds for any $x \in (a, b)$ (cf. Section 3.3). For the sole purpose of constructing the mean value curve, the abscissa of the mean value $f(c)$ can be approximated by a midpoint $d = (b - a)/2$.

3.4. Topological analysis of the pointwise subtraction of $h(t)$ from $q(t)$. The relation (8) reappears in Figure 3 illustrating its implementation to actual experimental data. Focusing on a single segment of $q(t)$, the figure represents topologic details of extracting of the oscillatory component $g(t)$ (in green) from the calorimetric time series $q(t)$ (in red). The single segment in Figure 3 A is delimited by the abscissa values t_1 and t_2 of the consecutive inflection points in $q(t)$, marked as red dots. The blue dot marks the point of coordinates (t^*, M) , with $t^* = (t_2 - t_1)/2$, which is the fit point for the interpolated curve $h(t)$ (in blue) to pass through in this segment. Note, that this fit point is shifted by Δt from the actual position t_M of the mean value M (an analogue to Δc in Figure 2). The resultant green line $g(t) = q(t) - h(t)$ is plotted against the right hand side axis y_2 , adjusted in such a way that the zero in the y_2 axis corresponds to M in the y axis, with both axes y and y_2 having the same scale. Physically, both the axes y and y_2 show the rate of heat evolution in mW units. Since $q(t)$ represents the rate of heat evolution as a function of time, so the red shading represents the total heat evolved during the period from t_1 to t_2 . The cyan shading illuminates the area between the curve $q(t)$ and the line $y = M$, yielded by integration of the difference $[q(t) - M]$ from t_1 to t_2 . Similarly to the analogous area in Figure 2, the “cyan area” in Figure 3 A is also divided into

two partitions, respectively within intervals (t_1, t^*) and (t^*, t_2) . Physically, it may be considered as a virtual flow of energy above and below the mean value level. Relation (8) applies and, accordingly, the areas of these (cyan) partitions in Figure 3 A are equal in absolute value, but opposite in sign. By virtue of (8), this must be true for each segment of the time series $q(t)$. So there is a detailed balance within each segment between the virtual energy production above and below the mean value. This is visualized by histograms in Figure 4 A and C. Each double bar represents a segment. The black half represents the integral of $[q(t) - M]$ within interval (t_1, t^*) , yielding the energy above the mean value M . The cyan half represents the absolute value of this integral within (t^*, t_2) , yielding the energy below M . The absolute values were used to enable visual comparability. In both histograms (respectively for the sorption of D_2 and H_2 in Pd), the pairwise black-cyan equivalence is evident for entire experiments. The exact data used to create the histograms in Figure 4 are listed in Tables I and II in columns (b) and (c). These data are an experimental manifestation of relation (8).

In Figure 3 B, the green shading have been added to accentuate the area under the extracted oscillations curve $g(t)$, plotted against the y_2 axis. Calorimetrically, it can be viewed as consisting of the exothermic and endothermic peaks, with respect to a now linear baseline, i.e., the $g(t) = 0$ line. A visual inspection suggests that the exo and endo “green” peaks should be topologically related to the positive and negative “cyan” lobes of the $[q(t) - M]$ area (the cyan shaded areas are mostly overlapped here, but fully visible in Figure 3 A). It can be shown that both the “cyan” and the “green” features are indeed approximately equal in their areas. But in order to prove this relation, we need first to identify an additional relation between the area of those green peaks, on one hand, and yet another feature, namely: the area enclosed between the segments of the curves $q(t)$ and $h(t)$ limited by points A and B marked in Figure 3 C.

Figure 3 C shows the groundwork of the pointwise subtraction of $h(t)$ from $q(t)$ demonstrated for a single segment AB. Note, that this operation can be viewed as a transformation of the area enclosed between the AB segments of the curves $q(t)$ and $h(t)$ into the area under the CD segment of the curve $g(t)$ (plotted against the y_2 axis). Each point in the $q(t)$ curve (red crosses) undergoes a vertical shift (downward or upward) to a new position, forming the new curve $g(t)$ (green open dots). It can be shown, that for any point X in the AB segment of the curve $q(t)$, the absolute value of its shift $|q(t_x) - g(t_x)|$ (upward or downward) to its new position X' in the CD segment of $g(t)$ is a linear function of its abscissa t_x within the interval $[t_A, t_B]$. The index “x” indicates, that the variable t_x is only defined within a single segment. In fact, each point in the area between the graphs $q(t)$ and $h(t)$ undergoes such shift, to form the area under the $g(t)$. Therefore, for any such point, having the abscissa $t_x \in [t_A, t_B]$, the pointwise subtraction can be written as

$$g(t_x) = q(t_x) - h(t_x) \quad (12)$$

Note, that the AB segment of $h(t)$ can be approximated as a straight line. Therefore, since $h(t_x)/(t^* - t_x) = \text{tg}\theta$, and using the approximating $\text{tg}\theta = \theta$ we have

$$g(t_x) = q(t_x) - \theta(t^* - t_x) \quad (13)$$

so for any point t_x the difference between the corresponding values of the curves $q(t)$ and $g(t)$

is a linear function of t_x :

$$|q(t_x) - g(t_x)| = |-\theta t_x + \theta t^*|. \quad (14)$$

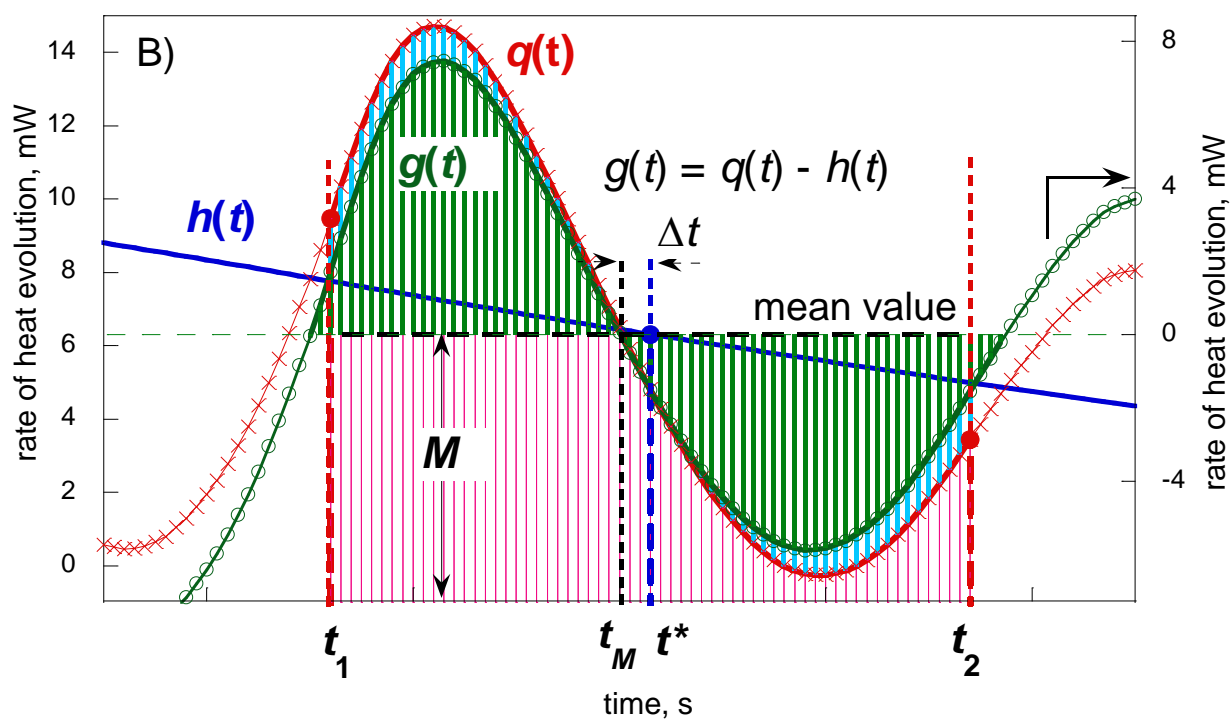
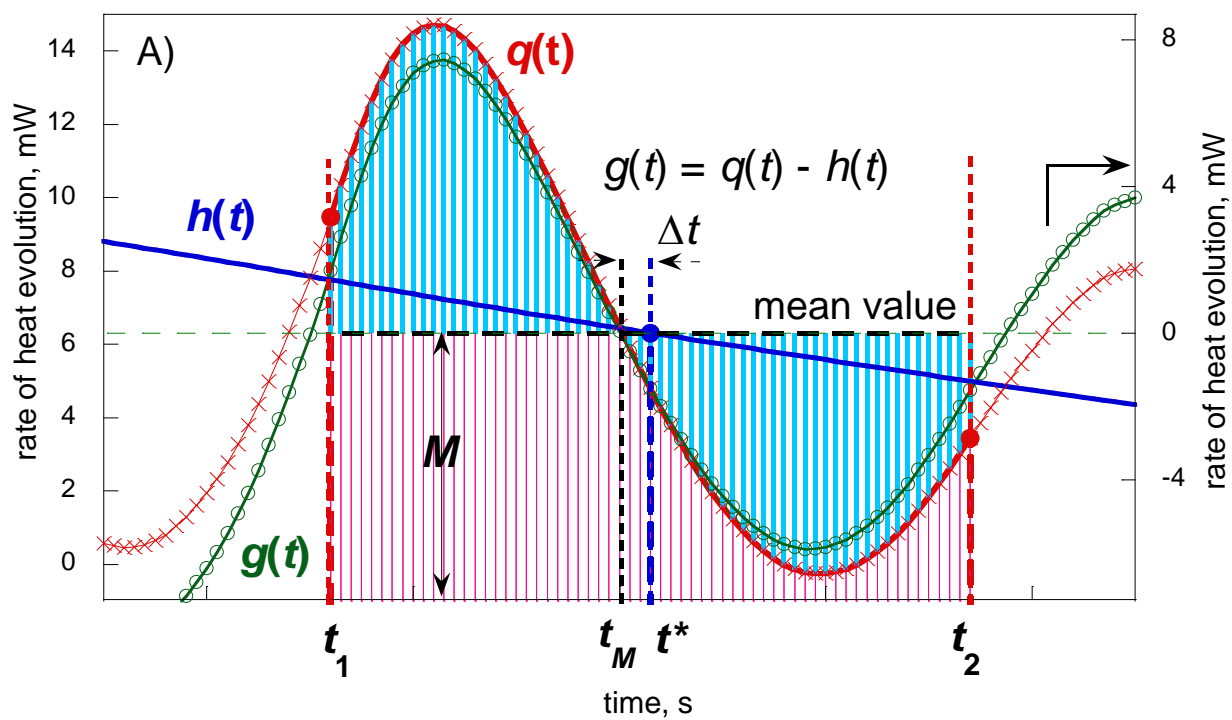
Hence the operation of the pointwise subtraction may in fact be viewed geometrically as a vertical shear of the area enclosed by the AB sections of the $h(t)$ and the $q(t)$, at a small shear angle $-\theta$. Accordingly, the abscissa is being preserved $t' = t$ and the ordinate transformed linearly $y' = -\theta t + y$. In matrix notation we have

$$\begin{bmatrix} t' \\ y' \end{bmatrix} = \begin{bmatrix} 1 & 0 \\ -\theta & 1 \end{bmatrix} \begin{bmatrix} t \\ y \end{bmatrix} \quad (15)$$

and since the determinant of the transformation matrix is one,

$$\left| \det \begin{bmatrix} 1 & 0 \\ -\theta & 1 \end{bmatrix} \right| = 1 \quad (16)$$

therefore the transformation in Figure 3 C is area preserving. It thus preserves the relations between the concave and convex partitions of the area enclosed by the AB sections of $q(t)$ and the AB section of $h(t)$ within the interval $[t_A, t_B]$. Now, the areas of these concave and convex partitions approximately correspond to the areas of the “cyan” lobes (positive and negative) within the interval $[t_1, t_2]$ in Figure 3 A and B. For small deviation between the limits of these intervals $[t_1, t_2]$ and $[t_A, t_B]$, this correspondence is close enough for relation (8) to hold also for the area enclosed by the AB sections of $q(t)$ and $h(t)$, and hence by virtue of (8) the concave and convex partitions are approximately equal to one another in absolute values. This relation, therefore, must be also preserved between the exo and endo peaks in the curve $g(t)$, as they are yielded by the area preserving vertical shear. Hence the important property of the resultant curve $g(t)$ turns out to be the pairwise equivalence of the subsequent exo- and endo-peaks, which also can be demonstrated experimentally (cf. Figure 4 B and D). In the Figure 4 B the filled plot of the $g(t)$ curve (green) is placed alongside the curve representing the integrals of $g(t)dt$ with variable upper limits (magenta). The total green area, that is, the sum of all exo and endo peaks in the $g(t)$ curve, is balanced to zero and this is reflected in the magenta line, i.e., the integral curve, reaching zero at the end. Remarkably, however, the magenta line hits the zero every time that a new period starts in $g(t)$, as it is illustrated in the enlarged fragment in Figure 4 D. This is an evidence of detailed exo/endo balance being kept in each individual period of the extracted oscillatory curve $g(t)$. Tables I and II list the exact values of the integrated exo and endo peaks in the curves $g(t)$ in columns (d) and (e).



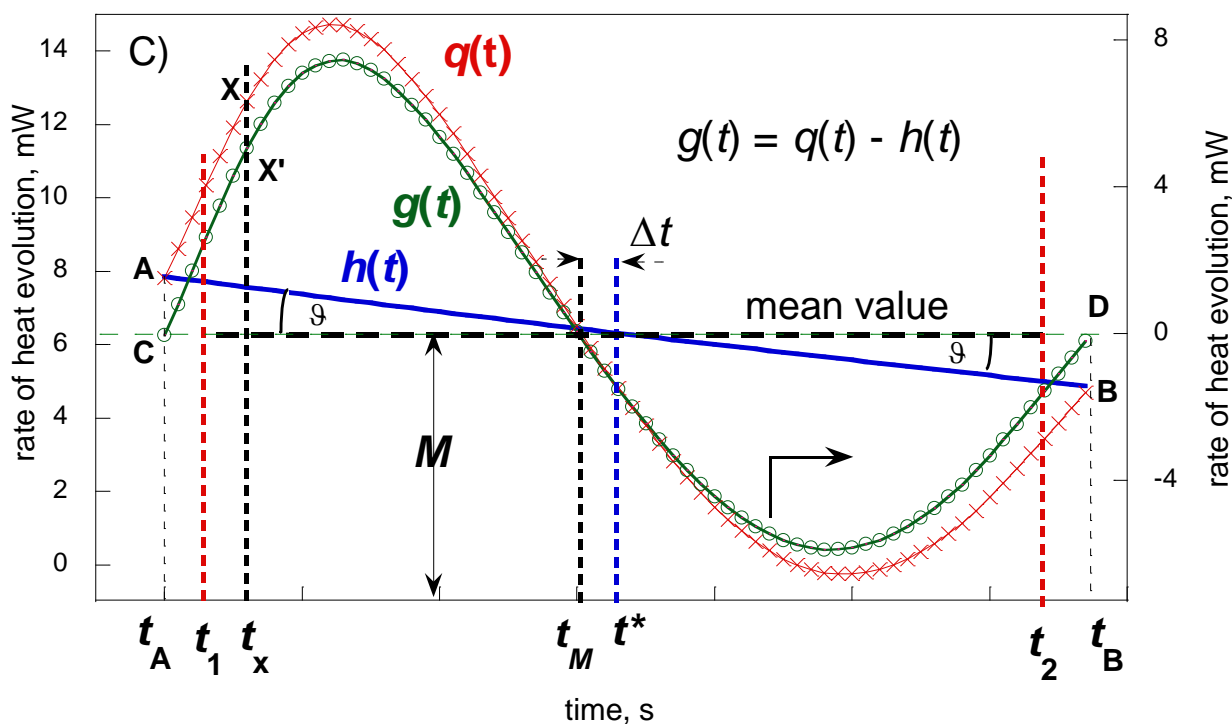


Figure 3. Topology of the pointwise subtraction of the approximated mean value curve $h(t)$ from the thermokinetic curve $q(t)$ illustrated for a single segment. **A)** The abscissa for the mean value M approximated as t^* and used to build the curve $h(t)$ subtracted from the $q(t)$. The “cyan” areas between $q(t)$ and the horizontal line $q = M$ are equal but of opposite signs. **B)** The affinity of the “cyan” areas to the “green” peaks of the extracted oscillatory curve $g(t)$. **C)** The $q(t) - h(t)$ subtraction may be viewed as a vertical shear of the area enclosed by the AB sections of the $h(t)$ and the $q(t)$, at a small shear angle $-\theta$, yielding the two peaks of the curve $g(t)$.

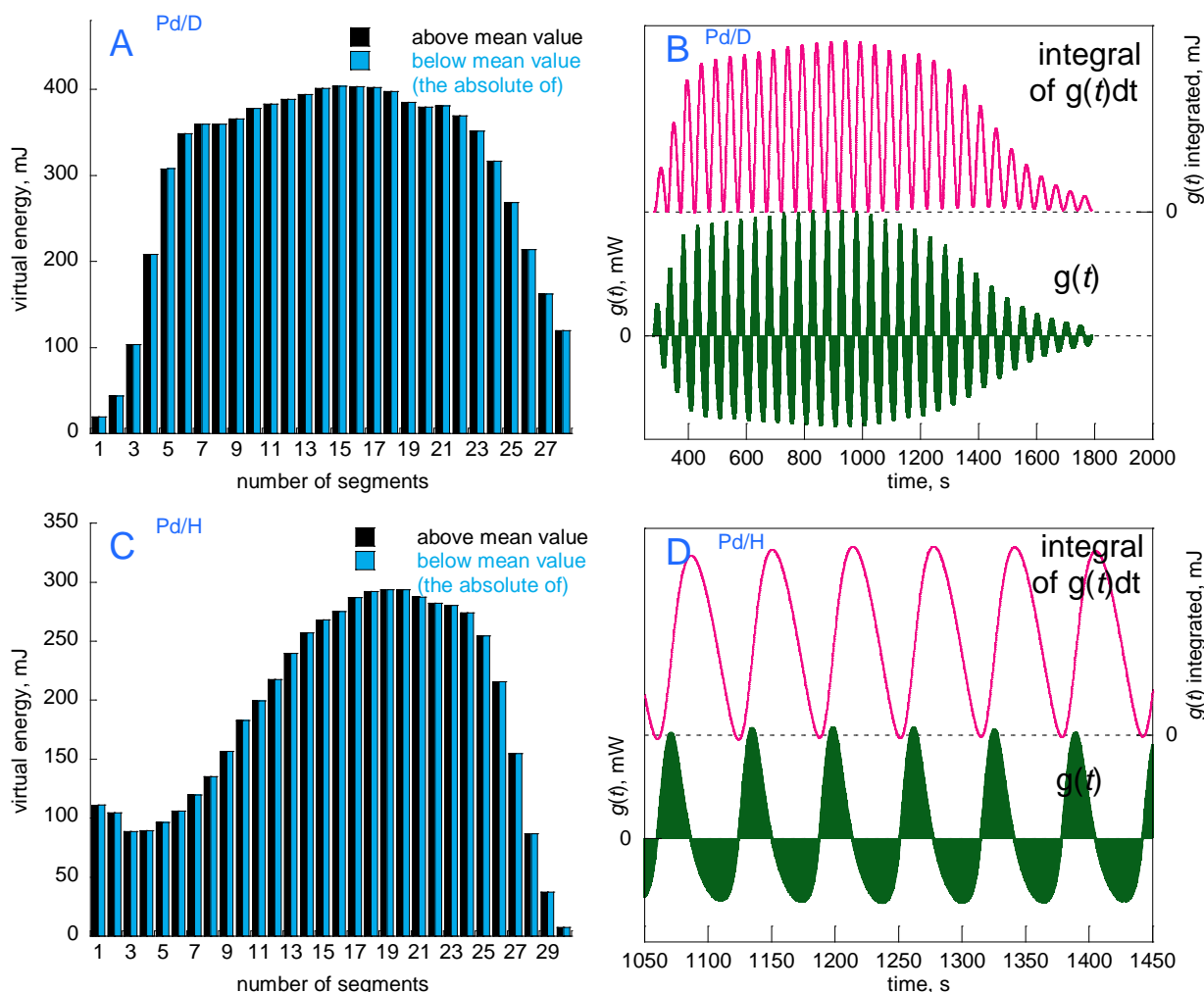


Figure 4. The experimental demonstration of formula (8). The histograms in panels **A** and **C** illustrate the equilibrium of the “cyan” partitions of Figure 3 A (i.e., the cyan shaded areas above and below the mean value M in Fig. 3 A) for the entire $q(t)$ curves in Pd/D₂ (panel **A**) and Pd/H₂ (panel **C**). Each of the black/cyan double bars corresponds to a single segment of $q(t)$; for swift comparison, the cyan bars are in absolute values. The panels **B** and **D** show the extracted oscillatory curves $g(t)$ (green) along with their (cumulative) integrals with variable upper limit (magenta), evidencing the detailed exo/endo balance being maintained in each individual periods of the $g(t)$ curve. Panel **B** shows the entire Pd/D₂ sorption; panel **D** shows a 400 s fragment of the Pd/H₂ sorption.

4. Discussion.

The area under the oscillatory curve $g(t)$ is expectedly zero, within a numerical/experimental error. Mathematically, this is the result of the fact that the areas under both the curves $q(t)$ and $h(t)$ are equal (cf. Figures 1A, B). Physically, this is because the total heat to evolve in the sorption process is invariant. The nonlinear kinetics that manifests itself in the oscillating rate of heat evolution cannot change the reaction thermodynamics and, therefore, cannot change the total amount of heat evolved in the reaction. Thus the $g(t)$ curve only extracts the oscillatory component from the thermokinetic time series in a way preserving the total evolved heat. The area under the $g(t)$ curve must eventually sum up to zero (cf. Figure 4 B), since this is necessary for thermodynamic foundation of the reaction to be preserved.

Apart from the total balance, however, there is also maintained a detailed balance of energy within each individual oscillatory period. Figure 3 B illustrates this effect for a single period, evidenced by the equivalence of the green shaded areas; Figures 4 B and D demonstrate the pairwise equivalence of exo- and endo-peaks in the entire $g(t)$ curves. Mathematically, this pairwise equivalence is the consequence of relation (8). Physically, it is related to the technical details of the discretization that was applied to the experimental time series $q(t)$. In this regard, it is an effect of using the inflection points to define the limits of the oscillatory periods in the $q(t)$ curve, for which subsequently the mean values were individually calculated. Adopting this procedure was dictated by our previous experience with the Pd/H system, suggesting that the positions of inflection points in the thermokinetic oscillations are closely related to the mechanism of the oscillatory sorption. In particular, in the experiments using the potentiostatic and the microcalorimetric method combined, we found that the variations of the electric current in the Pd sample measured *in situ* on its exposure to hydrogen, correlated with the periodicity of the accompanying heat evolution.⁵ We recorded strong electric perturbations coinciding with the concave downward parts of the oscillatory heat evolution, whereas the convex (concave upward) parts, in contrast, only saw a stable current in the Pd powder. Crucially, the electric perturbations were roughly spanning the intervals between the inflection points of the thermokinetic time series (cf. Fig. 5 in ref. 5). Thus the electrical instabilities turned out to be associated exclusively with the events of intense heat production. During the less energetic episodes, on the other hand, the current was not disturbed. It has been concluded, that the thermokinetic oscillations reflects a two-step mechanism of which only the first step involves a high rate production of energy, but occurs alternately with the second a less energetic one. Apparently, these two steps are reflected in the pairwise structure of the oscillatory curve $g(t)$. Their different exothermicity are related to the detailed exo/endo balance within each period of the $g(t)$ oscillations. Still there remains an open question, as for the nature of a book-keeping mechanism that must be active throughout the entire oscillatory sorption, making sure that the detailed balance of the oscillatory component of energy is being maintained in each individual period of oscillations. While the exact nature of this mechanism is not known, nevertheless certain features of it may be postulated. First, that it is acting in a short range. Second, that it must support synchronization of a body of micro-oscillators.

As for being short-ranged, it may be argued, that the book-keeping mechanism has to keep track of the expenditure of the oscillatory energy apparently without using any memory. Likely, therefore, it is operating at a rather elementary level, i.e., that of single Pd particles, or, even more underlying, a level of μm -size domains. In fact, the formation of domains turns out to be often accompanying oscillations in chemical reactions and this notion is now supported by a considerable body of research.⁸⁻¹⁴ Also the mechanism postulated in ref. 5 rationalizes the oscillatory heat evolution in terms of the domain formation on the Pd surface. Accordingly, these domains contain the adsorbed molecules of H_2 , and the periodicity of sorption results from a criticality of the dissociation of the adsorbed $\text{H}_{2\text{ads}}$ molecules into the atomic hydrogen species. It means, that it requires a certain critical amount of $\text{H}_{2\text{ads}}$ to be accumulated in a domain to initiate their dissociation. Once initiated, the dissociation process is fast and energetic and it is thus responsible for the exothermic peaks in the thermokinetic oscillations. The intermittent periods of adsorption and accumulation of $\text{H}_{2\text{ads}}$, on the other hand, correspond to the periodic lack of heat production (and also to the stability of electric current). Within this framework, it should be enough for the book-keeping mechanism to be operative over a short range, actually corresponding to a μm -size domain on the Pd surface.

A synchronization of those Pd domains, viewed as micro-oscillators, is yet another aspect that seems to confirm the operation of the book-keeping mechanism at elementary level. The model proposed in ref. 5 involves the periodicity as an intrinsic facet of the reaction mechanism, indicating that the thermokinetic oscillations are native to the process of sorption, rather than being induced by any external interference. If, in spite of this, the oscillatory kinetics in the Pd/H system is being detected rather occasionally, it is in fact a deficit of the synchronization that is to be blamed for that scarcity. The powdered Pd sample exposed to hydrogen consists of a large number of metallic particles, each of them reacting individually. The thermokinetic oscillations of such powdered sample can only be detected and measured if the oscillations in the individual domains are phase-synchronized. This means, that they all must oscillate with the same frequency. We reiterate, that the sorption of hydrogen in each domain proceeds in a series of successive uptakes, each accompanied by a heat evolution episode, and that the rate of the two are strictly related.⁵ The synchronization of both those rates between all the domains is necessary for the thermokinetic oscillations to be detected macro-kinetically, that is, for the oscillatory curves such as the $q(t)$ to be recorded and for the $g(t)$ to be subsequently extracted. Arguably, the equivalence of the successive exo and endo peaks in the $g(t)$ curve must also be maintained micro-kinetically. That is, the same detailed balance as that found in $g(t)$ must be also maintained at a level of single domains, in order to make the synchronization possible. An alternative would be seeing the mutual proportions of the exo and endo effects varying broadly from one domain to another. This would effectively prevent any synchronization, since reaching equal frequencies in all domains would not be possible without having the exo and endo effects microbalanced within each single domain. Hence the book-keeping mechanism implementing the formula (8) may expectedly be acting at a level as elementary as that of single domains in order to support their synchronization. A likely coupling medium for the synchronization seems to be the gas phase: indeed, the periodic pressure changes of the same frequency as that of the thermokinetic oscillations has been recorded during sorption of hydrogen in Pd.³

The oscillatory process should therefore involve not only the breaking of time symmetry, which is the oscillatory kinetics itself, but also the domain formation on the Pd surface, which amounts to breaking of space symmetry. As it involves both the periodicity and the domain formation on the Pd surface, so the proposed mechanism contains the physical symmetry breaking elements that may be conducive to the system's implementation of the mathematical properties of the oscillatory time series such as $q(t)$ and $g(t)$ expressed as formula (8) and confirmed experimentally (cf. Figure 4).

5. Conclusions.

A mathematically rigorous method has been proposed to extract a pure oscillatory component from periodic time series recorded in oscillatory reactions that occur far from equilibrium. The concept was implemented using thermokinetic time series recorded microcalorimetrically in the oscillatory sorption of hydrogen and deuterium in Pd. Following discretization of the original data, the mean value theorem for integrals makes it possible to calculate a range of mean values, one for each individual period of thermokinetic time series. The obtained sequence is subsequently used as fit points to construct a flat curve modeling a hypothetical non-oscillatory heat evolution under otherwise the same reaction conditions. Crucially, the areas under both curves, i.e., the modeled flat and the experimental oscillatory one, are the same, attesting to the method's validity. This is due to the invariance of the molar heat of reaction, irrespective of whether the oscillations occur or not. The pointwise subtraction of this modeled bas-line from the original curve yields a new time series representing the extracted oscillatory component. Since this new time series oscillates around the abscissa axis, so it is now possible to analyze the thermokinetic oscillations in terms of a succession of alternating exo and endo thermal effects. It reveals a pairwise exo/endo equivalence, i.e., each exo peak is followed by an endo peak that have the same area but of opposite sign. Hence, apart from whole the extracted oscillatory time series yielding zero on integration, also the exo and endo effects equilibrate one another within each period individually. This detailed exo/endo balance is a reflection of the mathematical relation expressed in equation (8). Physically, it seems to reflect a book-keeping mechanism operative at a very elementary level of the μm -size domains, viewed as micro-oscillators of which formation and synchronization enable the oscillatory kinetics of the sorption process to be calorimetrically detectable in macro scale.

Table I. Pd/D₂ results: (a) The mean values obtained for successive segments of the thermokinetic oscillations $q(t)$, used to construct the approximated mean value curve $h(t)$ shown in Figure 1 A (in blue). The values in columns (b) and (c) correspond to the black and cyan bars of histogram in Figure 4 A. The values in columns (d) and (e) represent the areas of the exo and endo peaks of the extracted oscillatory curve $g(t)$ shown (in green) in Figures 1E and 4 B.

(a) Pd/D ₂ Mean value, mW	(b) Partitions above mean value, mJ	(c) Partitions below mean value, mJ	(d) Exo peaks in $g(t)$, mJ	(e) Endo peaks in $g(t)$, mJ
27.577	19.081	-19.099		
27.508	43.517	-43.496		
27.252	103.11	-103.13	107.09	-107.44
26.780	208.22	-208.21	215.89	-217.54
27.450	307.68	-307.70	320.72	-320.98
28.638	348.20	-348.19	361.32	-358.24
29.176	359.50	-359.50	368.39	-368.20
29.468	359.50	-359.50	373.92	-373.87
29.810	365.86	-365.87	379.84	-380.97
30.074	377.98	-378.00	385.92	-385.59
30.430	382.93	-382.91	392.00	-391.55
30.768	388.32	-388.33	398.90	-398.93
31.106	394.16	-394.15	402.85	-403.84
31.348	400.85	-400.85	408.81	-408.66
31.585	403.61	-403.60	411.58	-410.86
31.693	403.02	-403.03	412.66	-412.16
31.752	402.01	-402.02	410.27	-410.36
31.488	397.43	-397.45	402.33	-400.68
30.884	385.05	-385.03	386.86	-384.11
29.305	379.34	-379.32	375.29	-373.52
27.174	380.89	-380.87	374.36	-374.61
24.928	369.10	-369.10	358.95	-357.18
22.021	351.28	-351.26	334.87	-334.31
18.706	316.39	-316.41	296.27	-293.85
14.875	268.55	-268.56	245.18	-244.76
10.987	213.91	-213.93	190.26	-191.65
7.5472	162.19	-162.19	142.15	-144.50
4.9702	119.70	-119.70	105.56	-107.30

Table II. Pd/H₂ results: (a) The mean values obtained for successive segments of the thermokinetic oscillations $q(t)$, used to construct the approximated mean value curve $h(t)$ shown in Figure 1 B (in blue). The values in columns (b) and (c) correspond to the black and cyan bars of histogram in Figure 4 C. The values in columns (d) and (e) represent the areas of successive exo and endo peaks of the extracted oscillatory curve $g(t)$ shown (in green) in Figures 1 F and 4 D (fragment).

(a) Pd/H ₂ Mean value, mW	(b) Partitions above mean value, mJ	(c) Partitions below mean value, mJ	(d) Exo peaks in $g(t)$, mJ	(e) Endo peaks in $g(t)$, mJ
18.452	111.02	-111.05	112.73	-109.90
17.999	104.59	-104.59	102.71	-102.45
17.397	88.786	-88.785	87.133	-89.662
17.129	89.284	-89.258	90.893	-91.493
16.899	96.520	-96.549	99.087	-99.157
16.829	106.14	-106.11	109.60	-110.93
16.687	119.78	-119.77	126.80	-127.45
16.618	135.04	-135.03	145.35	-147.52
16.483	156.57	-156.54	169.65	-167.47
16.527	182.67	-182.67	194.61	-195.37
16.550	199.62	-199.59	218.07	-221.94
16.502	217.42	-217.44	244.23	-244.12
16.574	239.80	-239.78	268.02	-266.41
16.754	257.10	-257.08	286.10	-286.97
16.937	267.86	-267.88	300.47	-301.30
17.153	275.08	-275.06	310.75	-311.79
17.534	286.96	-286.97	321.92	-318.38
17.792	291.92	-291.95	323.31	-324.40
17.819	293.46	-293.43	324.70	-322.18
17.912	293.61	-293.64	320.99	-321.35
17.853	287.47	-287.44	314.75	-314.11
17.271	282.04	-282.06	306.08	-303.88
15.929	280.39	-280.39	298.02	-294.92
14.305	274.13	-274.11	284.60	-283.76
12.179	254.27	-254.24	258.71	-256.42
9.3355	215.55	-215.54	208.83	-205.80
6.3099	154.82	-154.82	136.64	-139.20
3.7687	86.673	-86.671	70.203	-74.440
2.0762	37.262	-37.264	30.542	-32.475
1.3049	7.4657	-7.4675		

Acknowledgements

The authors acknowledge the financial support of the National Centre of Science (National Science Centre, Poland, grant no. 2012/07/B/ST4/00518) as well as the support and assistance of Microsca Energy Technology Ltd (Thatcham, UK).

Data Availability

The data that support the findings of this study are available from the corresponding author upon reasonable request.

References

1. I. Prigogine, G. Nicolis, On Symmetry-Breaking Instabilities in Dissipative Systems, *J. Chem. Phys.*, 1976, 46, 3542-3550.
2. E. Lalik, J. Haber, A. J. Groszek, Oscillatory Rates of Heat Evolution during Sorption of Hydrogen in Palladium *J. Phys. Chem. C*, 2008, 112, 18483-18492.
3. E. Lalik, An empirical dependence of frequency in the oscillatory sorption of H₂ and D₂ in Pd on the first ionization potential of noble gases, *J. Chem. Phys.*, 2011, 135, 064702.
4. E. Lalik, Chaos in Oscillatory Sorption of Hydrogen in Palladium, *J. Math. Chem.*, 2014, 52, 2183–2196.
5. E. Lalik, G. Mordarski, R. P. Socha and A. Drelinkiewicz, Chaotic variations of electrical conductance in powdered Pd correlating with oscillatory sorption of D₂, *Phys. Chem. Chem. Phys.*, 2017, 19, 7040-7053.
6. E. Lalik, R. Mirek, J. Rakoczy, A. Groszek, Microcalorimetric study of sorption of water and ethanol in zeolites 3A and 5A, *Catal. Today*, 2006, 114, 242-247.
7. P. K. Sahoo, T. Riedel, Mean value theorems and functional equations, World Scientific Publishing Co. Pte. Ltd., Singapore, New Jersey, London, Hong Kong, 1998, p. 208.
8. S. Jakubith, H. H. Rotermund, W. Engel, A. von Oertzen, G. Ertl, Spatiotemporal Concentration Patterns in a Surface Reaction: Propagating and Standing Waves, Rotating Spirals, and Turbulence, *Phys. Rev. Lett.*, 1990, 65, 3013-3016.
9. R. Imbihl, S. Ladas, G. Ertl, Spatial coupling of autonomous kinetic oscillations in the catalytic CO oxidation on Pt(110), *Surf. Sci.*, 1989, 215, L307-L315.
10. M. Eiswirth, P. Möller, K. Wetzl, R. Imbihl, G. Ertl, Mechanisms of spatial self-organization in isothermal kinetic oscillations during the catalytic CO oxidation on Pt single crystal surfaces, *J. Chem. Phys.*, 1989, 90, 510-521.
11. J Wolff, H H Rotermund, Local periodic forcing of CO oxidation on a Pt(110) surface, *New J. Phys.*, 2003, 5, 60.
12. M. D. Graham, M. Bar, I. G. Kevrekidis, K. Asakura, J. Lauterbach, H. H. Rotermund, G. Ertl, Catalysis on microstructured surfaces: Pattern formation during CO oxidation in complex Pt domains, *Phys. Rev. E*, 1995, 25, 76 – 92.
13. J. Halatek, E. Frey, Rethinking pattern formation in reaction–diffusion systems, *Nat. Phys.*, 2018, 14, 507–514.
14. Y. Suchorski, M. Datler, I. Bepalov, J. Zeininger, M. Stöger-Pollach, J. Bernardi, H.k Grönbeck, G. Rupprechter, Visualizing catalyst heterogeneity by a multifrequential oscillating reaction, *Nature Communications*, 2018, 9, 600.